Letters in High Energy Physics
ISSN: 2632-2714
Volume 2024

# Restriction of Oxygen Vacancy in Oxygen-Deficient Srtio$_3$ Via Substitution Dopants in B Site: Density Functional Theory Calculations.

**Anwar Nazar Hussein [1,2, a], Raied A. S. AL-Hamadany [2,b], M. T. Ahmadi [1,c]**

[1]PhD student in the Physics department, Faculty of Science, Urmia University, Urmia, Iran.
[2] Department of Physics, College of Education for Pure Sciences, University of Thi-Qar, Thi-Qar, 64001, Iraq.
[a]e-mail: anwar.nazar@utq.edu.iq (Corresponding author)
[b]e-mail: raid.abass.eps@utq.edu.iq
[c]e-mail: mt.ahmadi@urmia.ac.ir

**ABSTRACT:**

Capacitors and gate dielectrics are just two examples of when strontium titanate's ($SrTiO_3$) dielectric properties would be helpful. Unintentional oxygen vacancy in as-grown $SrTiO_3$ during growth conditions makes it electrically active due to positively charged oxygen vacancy which is more stable than its neutral form. Controlling of the electrical activity of $V_o$ is an importance to tailor the electrical feature of $SrTiO_3$. The electrical and structural characteristics of metal-doped $SrTiO_3$ have been investigated using First-principal simulation. Mg, Ni and Cu have been incorporated as substitutions for Ti, in oxygen-deficient $SrTiO_3$. Inherent Oxygen vacancy forms strong binding with dopant substituting Ti with binding energy up to 4.41±0.09 eV for $Cu_{Ti}$-$V_o$ complex. $M_{Ti}$ and more specifically $Cu_{Ti}$ could help counteract or capture the $V_o$ effect in as-grown $SrTiO_3$. Doping with dopants that act as electron captures could be the effective and reliable route to confine electrically active $V_o$ in $SrTiO_3$

**Keywords:** DFT; SrTiO3; Oxygen vacancy; Transition metal; Binding Energy.

## 1. Introduction

Due to their exceptional physical and organic characteristics, ferroelectrics made from perovskite have garnered significant interest from researchers for their potential applications in semiconductor technology. The incorporation of impurity atoms and deviations from harmonious chemical makeup even in materials that are nominally pure-can substantially influence various properties, including electrical (dielectric characteristics and electrical conductivity), magnetic, optical, thermal, and other properties. Furthermore, the intentional modification of material properties is a critical area of investigation. One technological approach involves the planning and creation of structural defects, such as inherent defects, defects induced by radiation, and those introduced by impure atoms, which can modulate specific material properties across a considerable range. In particular, the examination of substitution point defects in A and B sites of strontium titanate ($SrTiO_3$) is of great interest. Strontium titanate serves as a prototypical material within the perovskite family. [1, 2].

$SrTiO_3$ is one of the most interesting ternary perovskite oxides [3]. The crystal structure of $SrTiO_3$ is cubic at room temperature with space group symmetry *Pm3m* [4]. In the cubic phase, all of the atoms in the structure (Sr, Ti, and O) are in their high symmetry sites. However, at low temperatures, the crystal structure undergoes cubic to tetragonal phase transition [5]. The tetragonal phase of $SrTiO_3$ is characterized by rotation of neighbouring oxygen sub-lattices opposite to each other around [001] direction. The angle of rotation has been reported in previous measured to be 2.00$^o$ [6] and 2.01$^o$ [7]. Theoretical investigation procedures adopted in this study reflect well the angle of oxygen sub-lattices twisting at round 1.98$^o$. Other theoretical study produces value of angle 1.95$^o$ [8] and this result agrees well with this calculated value as well as with those measured from experiments. $SrTiO_3$ has an interesting electronic, electrical, optical, and dielectric properties. It has density around 5.12 gm/cm$^3$ [9], refractive index within the range 2.32 – 2.37 [10], melting point 2075 $^o$C and thermal expansion co-effeicient 9.4*10$^{-6}$/$^o$C [11]. In addition to these

properties and more interestedly, the dielectric properties are highlighted by high dielectric constant at around 300 [12]. The high dielectric constants of $SrTiO_3$ in comparison with other perovskites for instance $ZrTiO_4$ , BiTiO, $CoTiO_3$ , TiTaO, [13,14] make this material convenient for wide range of applications. These applications are including; metal-oxide semiconductor field effective transistor (MOSFET) [15], negative capacitor [16], resistive switching[17] dielectric random-access memory (DRAM) [18]. Despite the unique dielectric functionality of $SrTiO_3$, it shows a limitation in many applications as dielectric substance. These drawbacks are highlighted by the leakage current occurs during the application of $SrTiO_3$ as a dielectric. This means that as-grown $SrTiO_3$ has conductivity despite its dielectric properties. Wide range of both experimental and theoretical studies in the literature have been carried out to understand the main reason behind this limitation and overcome this drawback[19]. The majority of these investigations were focusing on impact of native defect on the electrical properties of $SrTiO_3$ [20]. Oxygen vacancy has gained a high focusing and investigation in comparison to other native defects. Oxygen vacancy was the focus of interest mainly due to its formation energy specially in the ionized form [21]. The undesirable leakage current and interested resistive switching are still an area of interest. Therefore, controlling and tailoring oxygen vacancy in term of its formation, migration and binding with other defects becomes an interest of investigation practically and computationally.

Various deposition approaches have been employed to fabricate thin films of $SrTiO_3$; however, organic precursors are frequently employed and cause contaminants impurities [22]. As known that growth of crystalline $SrTiO_3$ is driven by environment of growth condition of elements included in the process. This implies that $SrTiO_3$ might be grown under either oxygen rich or oxygen poor conditions. Similarly, the growth could be under metal-rich or lean conditions. Based on growth conditions of $SrTiO_3$, oxygen vacancy is the most probable defect that formed under anion reduction conditions in comparison with other native defects, including titanium vacancy, strontium vacancy, titanium interstitial, strontium interstitial and oxygen interstitial [23]. The low formation energy of $V_o$ makes it hardly avoidable defect in as grown $SrTiO_3$. Previous investigation reported formation energy of oxygen vacancy to be around 2 eV. According to another theoretical investigation adopted density functional calculation, the formation energy was calculated to be between 1.0 to 1.6 eV [24]. In addition to calculated value of formation energy, the study demonstrates that the cell size is a critical parameter for quantitative assessment of formation energy. In addition to its low formation energy in bulk $SrTiO_3$, oxygen vacancy is energetically favorable to be formed at the surface of $SrTiO_3$. For $TiO_2$ termination surface of $SrTiO_3$, the previously documented value of formation energy was 7.62 eV for non-ionized vacancy and 4.77 for singly ionized vacancy [25]. The missing of oxygen ion to create oxygen vacancy in $SrTiO_3$ yields two electrons in $SrTiO_3$ system that hosting the vacancy. Therefore, the vacancy will be existing in neutral form as well as single and double positively charge states. i.e. in 0, +1 and +2 charge states. Considerable investigations report that the oxygen vacancy is more stable in the +2-charge state [26]. Thus, the stabilization of doubly ionized form of the vacancy implies that $SrTiO_3$ has an electrical activity. Consequently, the formation of oxygen vacancy in +2 charge state will effectively affect the dielectric functionality of $SrTiO_3$ in many of its applications. It is well known that native defects, including oxygen vacancies ($V_o$), have a significant impact on the physical properties of $SrTiO_3$ because they produce localized electronic states in the band gap [27], which causes as-grown $SrTiO_3$ to display n-type conductivity. There is a strong anisotropic diffusion of $V_o$ in the case of strained ferroelectric $SrTiO_3$. Leakage imbalance in capacitors is thought to be caused by interactions and vacancies being trapped by other defects at the interfaces; $V_o$ is a crucial defect in resistance switching phenomena [29–31]. Since reducing leakage current is essential in capacitors, this electrical conductivity poses serious issues [28]. A direct nearest-neighbor hopping mechanism facilitates the migration of oxygen vacancies along the lattice in both ferroelectric in nature (strained) and antiferroelectric (unstrained) $SrTiO_3$ [30]. Moreover, metal impurities playing a major role as a trapping location for these vacancies, as it may selectively locate itself close to the electrode [31].

It is known that defects in materials might be bounded to each other to form a complex or might

be formed as individual defects. Therefore, binding anergy of complex in solids is significant quantity to assess the thermodynamic stability of complex. More significantly, valuable information can be obtained from binding energy to decide whether two defects are formed as individual separated systems or as complex in solids. Additionally, it provides quantitative estimate of the desired energy to overcome the force holding the two defects those forming the complex. Despite a growing body of evidence highlighting the role of metallic defects in $SrTiO_3$, the binding of native inherent $V_o$ and substitution dopant in A and B sites in the material remains a subject of limited exploration. Of particular interest is the possibility of transition metal dopants including Ni, Cu and Mg substitution for Ti serving as capturing sites for electrically active oxygen vacancies in $SrTiO_3$. This study aims to systematically investigate the structural, electrical, and optical properties associated with Ni, Cu, and Mg in $SrTiO_3$, with a focus on altering these properties through computational material design. First-principles simulations offer a reliable avenue for guiding experimental investigations. First-principles investigations have the capability to analyses the microscopic nature of crystallographic and electronic properties of materials those are limited to investigate using the practical techniques. It has been adopted as complementary procedure for wide range of experimental studies and in many cases, it was considered as a guidance for upcoming and expected experimental investigations.

In the research, we propose and investigate the probability of confining electrically active $V_o$ by doping substitution metal dopant to substitute Ti. Substitution defects are including Ni, Cu, and Mg. The idea of proposing these defects is producing electron captures defects in the vicinity of the oxygen vacancy in order to create charge balance in the system. We assess several structural and electrical features of doped $SrTiO_3$ and examine the binding interactions of $V_o$ oxygen vacancies with Ni, Cu, and Mg substituting B-site $SrTiO_3$. All calculations in this study were carried out by using density functional theory (DFT) simulations.

## 2. Computational Method and Models

Spin-polarised local density functional [32] computations were performed in the ab-initio modeling program code [33, 34] to study the structural and electronic characteristics of M-doped $SrTiO_3$. The structural features and binding energy of the oxygen vacancy in conjunction with dopants in Sr and Ti-sites have been studied.

The electron-ion interactions were simulated employing a norm-conserving Pseudopotential [35]. The valence configurations utilized for Sr, Ti, and O were $4s^24p^65s^2$, $3s^23p^63d^24s^2$, and $2s^22p^4$, respectively. Titanium, and oxygen were described using four sets of s-, p-, and d-Gaussian functions, resulting in a total of 40 functions per atom. These functions were employed to represent electronic wave functions using atom-centered Gaussian basis functions [36]. Using the Kohn-Sham potential and a plane-wave expansion of density, the Hamiltonian matrix elements were found [37], with a cutoff energy set at 300 Ha.

The computational method employed in our study yields an equilibrium lattice value of 3.88 ˚A for bulk $SrTiO_3$, which is consistent with prior results [38] and experiment [39]. The bulk modulus is also calculated to be $195*10^6$ Nt/mm$^2$. The calculated value of bulk modulus in good agreement with $222*10^6$ Nt/mm$^2$ form experimental study [40] and $174*10^6$ Nt/mm$^2$ from theory [41]. The enthalpy of formation of $SrTiO_3$ calculated using the current approach is -3.60 eV/atom which is in a line with -3.46 eV/atom from experiment [42]. The well accordance of these calculated parameters with previous literatures provide benchmark for other calculations in our study. Furthermore, a similar computational approach has been successfully adopted to explore the oxygen vacancy migration under bi-axial tensile,[43] compressive strain, [44] as well as the electronic structure of the hydrated $SrTiO_3$ (001) surface [45].

The structural optimization process utilizes the conjugate gradients method to achieve optimized structures, ensuring that forces acting on each atom remain below $10^{-3}$ atomic unit. In the final phase, a reduction in total energy to below $10^{-5}$ Ha is sought to establish equilibrium structures. Allowing all atoms to move freely is crucial in determining these equilibrium configurations.

Additionally, symmetry constraint conditions are circumvented during the optimization process by evaluating the energy of each defect structure about the lattice symmetry. This implies that the hosted defect might be

constrained due to maintenance of symmetry, thus, for each system under investigation, the symmetry was perturbated to produce high degree of optimization. Defects are modeled using a 160-atom supercell with lattice vectors defined as $2\sqrt{3}[a\bar{a}\bar{a}]$, $2\sqrt{3}[\bar{a}a\bar{a}]$ and $2\sqrt{3}[\bar{a}\bar{a}a]$, where $a$ represents the lattice constant of the primitive cubic cell. The 160-atoms cell size was created by double repeat of non-primitive 20-atoms cell size. The super cell adopted to model defective system compromise 32 formula unite of $SrTiO_3$. Therefore, for modelling of $Cu_{Ti}$, $Ni_{Ti}$, and $Mg_{Ti}$ systems, we adopted $Sr_{32}Ti_{31}CuO_{96}$, $Sr_{32}Ti_{31}NiO_{96}$, and $Sr_{32}Ti_{31}MgO_{96}$ respectively. Similarly, the modelling of complexes are $Sr_{32}Ti_{31}CuO_{96}$ for $Cu_{Ti}$-$V_o$, $Sr_{32}Ti_{31}NiO_{96}$ for $Ni_{Ti}$-$V_o$ and $Sr_{32}Ti_{31}MgO_{96}$ for $Mg_{Ti}$-$V_o$. The Brillouin zone is sampled utilizing a 2×2×2 Monkhorst-Pack mesh [46]. Higher sampling grid has been tested for more accurate results. We have tested 3×3×3 and found that the energy difference between 2×2×2 and 3×3×3 was negligible. The cell size was also converged by comparing the results from 160-atoms cell size with larger cell size containing 270 and 320 atoms. The difference in energy between 160-atoms and 207 atoms cell-size or 320 atoms cell-size was very small. Therefor, all the calculations in this study adopted 160-atoms cell size as it is less computational cost. The utilized cell size has been also adopted in previous calculation to investigate behaviour of other perovskite defective systems such as $BaTiO_3$ [43] and $PbTiO_3$ [47].

The Binding Energy of the complex M-$V_o$ is defined as the discrepancy in total energies between the individual components and the complex.

$$E^b(M,V_o) = E^T(M) + E^T(V_o) - E^T(M,V_o) - E^T{}_{pure}$$

Where the total energies of $V_o$ and M in their isolated forms are $E_T(V_o)$ and $E_T(M)$, respectively. The total energy of the complex is $E_T(M, V_o)$ and $E_{pure}$ for pure $SrTiO_3$. In the calculation of M–$V_o$ binding energies, different cell sizes have been adopted.

**3. Results and Discussion**

A series of calculations on the defect complex has been conducted to investigate the interactions between oxygen vacancies ($V_o$) and substitution dopant impurities (M). The binding energies for all configurations analyzed have been computed. Prior to the calculation of binding energy, structures containing individual defects (metal substitution Ti and oxygen vacancy) as well as structure containing the complex (two defect together) were optimized in advance. The optimization process for structures under investigation was converged with related parameter including sampling scheme of Brillouin zone.

The optimised structure with metal dopants instead of Ti is analyzed in term of bond lengths of dopants with surrounding oxygen ions. To begin, we will go over the optimised geometry, like the bonding in rock-salt, the six neighboring oxygen ions of $M_{Ti}$ (labelled (a) in Fig.1) are similar. Furthermore, it is observed that the distance between oxygen ions and dopants substituting for Ti is variant with respect to dopant identity. In contrast to bulk $SrTiO_3$, which has a bond length of 1.89 Å, the bond between any of $Cu_{Ti}$, $Ni_{Ti}$, and $Mg_{Ti}$ and the first neighbouring oxygen ions are slightly variant. The bond lengths of $Cu_{Ti}$, $Ni_{Ti}$, and $Mg_{Ti}$ with first nearest six oxygen ions are listed in Table.1.

Table.1 The bond lengths (in Å) between $Cu_{Ti}$, $Ni_{Ti}$ and $Mg_{Ti}$ and six surrounding oxygen ions labelled in Figure.1

| Structure | O1 | O2 | O3 | O4 | O5 | O6 |
|---|---|---|---|---|---|---|
| $Cu_{Ti}$ | 1.99 | 1.92 | 1.84 | 1.97 | 1.95 | 1.88 |
| $Ni_{Ti}$ | 1.89 | 1.86 | 2.65 | 1.86 | 1.89 | 2.65 |
| $Mg_{Ti}$ | 2.82 | 1.89 | 2.81 | 2.81 | 1.99 | 2.83 |

As clear from table.1, the inclusion of $Ni_{Ti}$ and is found to cause the lattice to tense due to the Ni-O bond lengths being shorter than host Ti-O bonds. It is obvious that there are four Ni-O bond lengths have the same order of length and an average of 1.875 Å, whereas the other two Ni-O bonds are longer in comparison with the other four bonds. In addition, these two bonds are longer than their equivalents Ti-O bonds in pure undoped systems. It means that inclusion of Ni dopant as substitution to

 

Ti will produces compression in four Ni-O bond lengths and tension in remaning two Ni-O bonds. The divergence of ionic radius of $Ni^{+2}$ (0.615Å) compared to $Ti^{+4}$ (0.68Å) is possible explanation for the tension. In case of Mg substituting Ti, it is clear $Mg_{Ti}$ relaxed by increasing the distance, hence the bond lengths between $Mg_{Ti}$ and the six connected oxygen ions. In contrast to $Ni_{Ti}$ the bond lengths of Mg-O are elongated in four Mg-O bonds with an average 2.82 Å, while the other two Mg-O bonds are 1.89 Å and 1.99 Å. The substitution of Ti with Mg is found to cause outward tension as clear form the divergence between Mg-O in the doped system and Ti-O in pristine $SrTiO_3$, where the former is longer in bond lengths. The elongation in four of Mg-O bond length in system containing $Mg_{Ti}$ is ascribed to nature of Mg-O in MgO which is equal to 2.30Å. In additions, ionic radius of $Mg^{+2}$ of 0.72Å might be the cause of local upward stress around $Mg_{Ti}$. The incorporation of Cu in Ti site yields comparable environment to bond length of Ti-O in pure $SrTiO_3$ despite the discrepancy in atomic radius between Cu (0.72 ) and Ti.

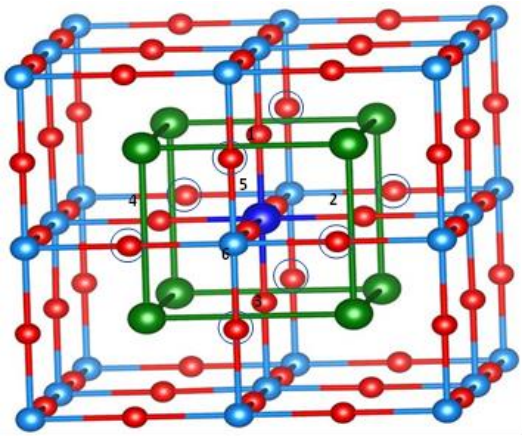


**Figure 1. shows the first nearest neighboure of oxygen ions laballed 1 to 6 and the second oxygen nearest neighbour oxygen ions highlighted with circles. The green, grey, red, and blue spheres symbolise Sr, Ti, O, and substitution dopant. The system is set up so that the vertical and horizontal directions are [001] and [100], respectively, with an off-axis presentation to improve understanding.**

Table.1 shows that bond lengths of Cu-O in case of Cu substation Ti have nearly similar bond lengths. The average order of Cu-O bond length is 1.92Å. The calculated average bond lengths are closer to identical Ti-O in pristine $SrTiO_3$. Therefore, it can conclude that structural perturbation caused by inclusion of Cu in Ti site is less in comparison with other dopants ($Ni_{Ti}$ and $Mg_{Ti}$).

In order to find the binding energy of $Cu_{Ti}$-$V_o$, $Ni_{Ti}$-$V_o$, and $Mg_{Ti}$-$V_o$ , systems composed of either $Cu_{Ti}$ or $Ni_{Ti}$ or $Mg_{Ti}$ and $V_o$ have, therefore, been modelled. In order to find the minimum energy structure of oxygen vacancy in the presence of substituted metal dopant. From geometrical and crystallographic perspectives of $SrTiO_3$, the oxygen ions can be categorized according the inter atomic distance separating the metal dopant (Ti in case pf pure $SrTiO_3$) into first, second, third… et. al. nearest neighbors. Hence, the oxygen vacancy could be located in the first, second, and third oxygen shells with respect to the metal dopant site. More progressively farther away from dopant site has also been considered and compared with other shells' sites. As clear from Figure.1 the metal (Cu, Ni, and Mg) dopant substitution Ti in $SrTiO_3$ has six oxygen ions labeled from 1 to 6 as first nearest neighbors. The second nearest neighbors of oxygen ions to the dopant are eight and highlighted with circles in figure.1. In addition, the third nearest neighbors of oxygen ions, all these sites have been tested to find the site with minimum energy. We observe that $V_o$ has an energy preference for the first adjacent oxygen shell, which means it misses one of the six oxygen ions linked to the dopant.

Using formula (1) and after optimization of all related structures of each complex in this study, the calculated binding energies of $Cu_{Ti}$-$V_o$, $Mg_{Ti}$-$V_o$ and $Ni_{Ti}$-$V_o$ are listed in Table.1

Table.1 : The binding energy (in eV) between oxygen vacancy and metal dopant substitution Ti ($Cu_{Ti}$-$V_o$, $Mg_{Ti}$-$V_o$ and $Ni_{Ti}$-$V_o$) in $SrTiO_3$

| Complex | $Cu_{Ti}$-$V_o$ | $Ni_{Ti}$-$V_o$ | $Mg_{Ti}$-$V_o$ |
|---|---|---|---|
| Binding energy (eV) | 4.41 | 2.60 | 3.91 |

As clear from the table the $Ni_{Ti}$-$V_o$ complex has lowest value of binding energy in comparison with other to complexes ($Cu_{Ti}$-$V_o$ and $Mg_{Ti}$-$V_o$). By contrast, $Mg_{Ti}$-$V_o$ has the highest value of binding energy. In general, and in comparison, with literatures, the computed binding energies of all complexes under investigations of dopants substituting Ti are greater than the previously published values for $Al_{Ti}$-$V_o$ (0.15 eV) [48] and $Fe_{Ti}$-$V_o$ (0.3-0.4 eV) [49]. The high values of binding energy are an outcome of charge imbalance between $Ti^{+4}$ and the dopants. The highest value has been found for $Cu_{Ti}$-$V_o$ complex. This implies that imbalance in valance state between $Ti^{+4}$ and $Cu^{+2}$ required charge compensation in the vicinity of $Cu_{Ti}^{-2}$. The binding with as grown $V_o^{+2}$ is the most probable route for compensation. Thus, high value can be ascribed to strong electrostatic interaction between $Cu_{Ti}^{-2}$ and the neighboring $V_o^{+2}$. The comparatively high binding observed in the case of $Cu_{Ti}$ inclusion as isolated acceptors, $Cu_{Ti}$ can be considered as a potential room temperature trap for $V_o$ in $SrTiO_3$. As previously indicated, $Cu_{Ti}$, $Ni_{Ti}$ and $Mg_{Ti}$ cause a local dilatation of the lattice with less pertibated in crystal structure for $Cu_{Ti}$. In specific $Cu_{Ti}$ can relax towards the vacancy in the complex and making it easier to accommodate the Cu ion. More specifically, the 2.15 Å and 1.76 Å axial Cu-O and Ti-O bond lengths, respectively, show that the relaxation of the ions linked to the vacancy is different. Furthermore, it is anticipated that this complex will be formed as a result of the electrostatic interactions. Since $V_o$ is a double donor, as is well-established in the literature, the combination can be characterized as $Cu_{Ti}^{2}$—$V_o^{+2}$. It is believed that this pair of acceptors and donors will form an isoelectronic defect and will be bound Coulombically. Further to the highest calculated value of binding energy for $Cu_{Ti}$-$V_o$, it is known that and as stated Vo has an energy barrier of migration being less in double ionized form, which implies that the vacancy required an energy to dissociate from the complex as well as an energy to overcome the energy barrier.

The binding energy magnitude of the reaction

$$M_{Ti} - V_o =\leftrightarrow M_{Ti}^{-2} + V_0^{+2}$$

Assuming the dissociation barrier is equal to the sum of the binding energy and the migration barrier of $V_o^{+2}$ (calculated at 0.72 eV) [50, 51], we arrive at a temperature of approximately 1800 K for a process that follows Boltzmann statistics, with a dissociation rate of 1 Hz and an attempt frequency of 16 THz. So, this may be seen as a ballpark figure for the growth temperature at which $Cu_{Ti}$ and an adjacent oxygen vacancy are likely to be integrated and the temperature at which annealing the material is required to activate the $Cu_{Ti}$ acceptors.

If $Cu_{Ti}$ is a double acceptor and, depending on the position of level in electronic structure, leads to *p*-type conductivity, it would make sense because Ti and Cu are expected to have different formal oxidation states at this site. Since $V_o$ generation is typically associated with as-grown *n*-type conductivity, an acceptor could be a way to remove the electrons produced from $V_o$.

## IV. CONCLUSIONS

Through the application of density functional theory, we conducted a study on the impact of replacing Ti with Cu, Ni, and Mg in $SrTiO_3$ on its geometrical properties. Our findings indicate that dopants induce variant local structural changes around the defect. The divergence in structural changes around the substituted dopant is lower for $Cu_{Ti}$ in comparison with other two structures ($Mg_{Ti}$ and $Ni_{Ti}$). The interaction between substitution dopants and the prevalent double donor oxygen vacancy shows high vales of binding energy for all system under study against those from previous investigations. In addition, the highest value of binding up to 4.41 eV has been obtained for $Cu_{Ti}$-$V_o$. Specifically, oxygen vacancies tend to favor the vicinity of the first oxygen shell and then localized near the substitution dopants. The resultant defect, electrically inert in nature, can be considered a pair of double acceptors and double donors, or in terms of crystal composition, as a local alloy comprising $SrTiO_3$, SrO, and CuO. For instance, in simulations using a 160-atom supercell, the defect-free system can be described as $(SrTiO3)_{32}$, while the defective system is represented as $(SrTiO_3)_{31}(SrO)(CuO)$. This implies that a stoichiometric CuO unit substitutes a native stoichiometric $TiO_2$ group. This system shows promise as a candidate for capturing oxygen vacancies due to its positive and high binding energy (4.41±0.09 eV), which is relatively high compared to previously studied Fe and Al substitutions. The binding of the $Cu_{Ti}$-Vo complex is expected to hold up to approximately 1800K.

**References**

1. Borstel G, Krumins A, Millers D. Defects and Surface-induced effects in advanced perovskites: Springer Science & Business Media; 2012.
2. Kvyatkovskii O. Quantum effects in incipient and low-temperature ferroelectrics (a review). Physics of the Solid State. 2001;43(8):1401-19.
3. N. Sai, A. M. Kolpak, and A. M. Rappe, "Ferroelectricity in ultrathin perovskite films," *Phys. Rev. B* **72**, p. 020101, 2005.
4. F. M. Ponter, E. J. H. Lee, E. R. Leite, and E. Longo, "High dielectric constant of SrTiO3 thin films prepared by chemical process," *J. Mater. Sci.* **35**, p. 4783, 2000.
5. C. Glover, M. E. Newton, P. Martineau, D. J. Twitchen, and J. M. Baker, "Hydrogen incorporation in diamond: The nitrogen-vacancy-hydrogen complex.," *Phys. Rev. Lett.* **90**, p. 185507, 2003.
6. F. L. Mattina, J. G. Bednorz, S. F. Alvarado, A. Shengelaya, K. A. Muller, and H. Keller, "Controlled oxygen vacancies and space correlation with Cr3 in SrTiO3," *Phys. Rev. B* **80**, p. 075122, 2009.
7. W. Gui-yun, Q. Ya, C. Jie, and W. Yan-ji, "Influence of Zn doping on the photocatalytic property of SrTiO3," *J. Fuel Chem. and Tech.* **38**, p. 502, 2010.
8. A. Sawa, "Resistive switching in transition metal oxides," *Materials Today* **11**, p. 28, 2008.
9. J. P. Goss, R. J. Eyre, and P. R. Briddon, "Bound substitutional impurity pairs in diamond: a density functional study," *J. Phys. Cond. Matter* **20**, p. 085217, Feb. 2008.
10. K. Bouzehouane, P. Woodall, B. Marcilhac, A. N. Khodan, D. Crete, E. Jacquet, J. C. Mage, and J. P. Contour, "Enhanced dielectric properties of SrTiO3 epitaxial thin film for," *Appl. Phys. Lett.* **80**, p. 109, 2002.
11. Y. G. Joh, H. D. Kim, B. Y. Kim, S. I. Woo, S. H. Moon, J. H. Cho, E. C. Kim, and C. C. R. Kim, D. H., "Effect of CoTiO3 formation on the magnetic properties of Co-doped TiO2 rutile," *J. Korean Physical Soc.* **44**, p. 360, 2004.
12. C. C. Wang and L. W. Zhang, "Dielectric behaviour of cobalt titanium oxide,"
13. *J. Phys. D* **40**, p. 6834, 2007.
14. K. Takemura, T. Sakuma, and Y. Miyasaka, "High dielectric constant (Ba,Sr)TiO3, thin films prepared on RuO2/sapphire," *Appl. Phys. Lett.* **64**, p. 2967, 1994.
15. G. D. Hu, S. H. Fan, C. H. Yang, and W. B. Wu, "Low leakage current and enhanced ferroelectric properties of Ti and Zn codoped BiFeO3 thin film," *Appl. Phys. Lett.* **92**, p. 192905, 2008.
16. K. C. Chiang, C. Huang, G. L. Chen, W. J. Chen, H. L. Kao, Y. Wu, A. Chin, and P. McAlister, "High-performance mim capacitors for analog applications," *IEEE Trans. Electron Devices* **53**, p. 2312, 2006.
17. R. Moazzam, "Ferroelectric thin film technology for semiconductor memory," *Semicond. Sci. Technol.* **10**, pp. 375–390, 1995.
18. S. H. Paek, E. S. Lee, S. H. Kim, and J. Y. Seong, "Control of the leakage current in SrTiO3 films by acceptor doping," **33**, p. 1239, 1998.
19. P. J. Kelly and R. D. Arnell, "Magnetron sputtering: a review of recent developments and applications," *Vacuum* **159**, p. 159, 2000.
20. A. Samanta, E. Weinan, and S. B. Zhang, "Method for defect stability diagram from *ab initio* calculations: A case study of SrTiO3," *Phys. Rev. B* **86**, p. 195107, 2012.
21. J. Lento and R. M. Nieminen, "Non-local screened-exchange calculations for defects in semiconductors," *J. Phys. Cond. Matter* **15**, pp. 4387–4395, 2003.
22. Lee SW, Han JH, Han S, Lee W, Jang JH, Seo M, et al. Atomic layer deposition of $SrTiO_3$ thin films with highly enhanced growth rate for ultrahigh density capacitors. Chemistry of Materials. 2011;23(8):2227-36.
23. W. Jiang, M. Noman, Y. M. Lu, J. A. Bain, P. A. Salvador, and M. Showronski, "Mobility of oxygen vacancy in SrTiO3 and its implications for oxygenmigration-

based resistance switching," *J. Appl. Phys.* **110**, p. 034509, 2011.

24. K. Eisenbeiser, J. M. Finder, Z. Yu, J. Ramdani, J. A. Curless, J. A. Hallmark, R. Droopad, W. J. Ooms, L. Salem, S. Bradshaw, and C. D. Overgaard, "Field effect transistors with SrTiO3 gate dielectric on si," *Appl. Phys. Lett.* **76**, p. 1324, 2000.
25. R. D. Leapman, L. A. Grunes, and P. L. Fejes, "Study of the L23 edges in the 3*d* transition metals and their oxides by electron-energy-loss spectroscopy with comparisons to theory," *Phys. Rev. B* **26**, p. 614, 1982.
26. E. Heifets, E. Kotomin, and V. A. Trepakov, "Calculations for antiferrodistortive phase of SrTiO3 perovskite: hybrid density functional study," *J. Phys. Cond. Matter* **18**, p. 4845, 2006.
27. P. I U, Shenoy US, Bhat DK. Nanocubic copper-doped $SrTiO_3$ for photoreduction of Cr (VI) and photodegradation of methyl violet. ACS Applied Nano Materials. 2023;6(18):16798-804.
28. Lee H, Lee K-C, Schunke J, Burton L. Leakage currents in multilayer ceramic capacitors. IEEE transactions on components, hybrids, and manufacturing technology. 1984;7(4):443-53.
29. Mojarad SA, Goss JP, Kwa KS, Zhou Z, Al-Hamadany RA, Appleby DJ, et al. Leakage current asymmetry and resistive switching behavior of $SrTiO_3$. Applied Physics Letters. 2012;101(17).
30. Mojarad SA, Kwa KS, Goss JP, Zhou Z, Ponon NK, Appleby DJ, et al. A comprehensive study on the leakage current mechanisms of Pt/$SrTiO_3$/Pt capacitor. Journal of Applied Physics. 2012;111(1).
31. Mojarad SA, Goss J, Kwa KS, Petrov PK, Zou B, Alford N, et al. Anomalous resistive switching phenomenon. Journal of Applied Physics. 2012;112(12).
32. Hartwigsen C, Gœdecker S, Hutter J. Relativistic separable dual-space Gaussian pseudopotentials from H to Rn. Physical Review B. 1998;58(7):3641.
33. Rayson MJ, Briddon PR. Rapid iterative method for electronic-structure eigenproblems using localised basis functions. Computer Physics Communications. 2008;178(2):128-34.
34. Perdew JP, Wang Y. Accurate and simple analytic representation of the electron-gas correlation energy. Physical review B. 1992;45(23):13244.
35. Drabold DA, Estreicher SK. Theory of defects in semiconductors: Springer; 2007.
36. Rayson M, Briddon P. Highly efficient method for Kohn-Sham density functional calculations of 500–10 000 atom systems. Physical Review B—Condensed Matter and Materials Physics. 2009;80(20):205104.
37. Yao Y, Fu H. Density-functional theory study of polarization saturation in strained ferroelectrics. Physical Review B—Condensed Matter and Materials Physics. 2009;80(3):035126.
38. Rabe KM, Ghosez P. First-principles studies of ferroelectric oxides. Physics of Ferroelectrics: A Modern Perspective: Springer; 2007. p. 117-74.
39. Yang Z, Zheng D, Yue X, Wang K, Hou Y, Dai W, et al. The synergy of Ni doping and oxygen vacancies over $CeO_2$ in visible light-assisted thermal catalytic methanation reaction. Applied Surface Science. 2023;615:156311.
40. C. Tang and R. Ramprasad, "Point defect chemistry in amorphous HfO2: Density functional theory calculations," *Phys. Rev. B* **81**, p. 161201, 2010.
41. J. X. Zheng, G. Ceder, and W. K. Chim, "First-principles study on the concentrations of native point defects in high-dielectric-constant binary oxide materials," **2**, pp. 227–229, 2008.
42. Aboub Z, Seddik T, Daoudi B, Boukraa A, Behera D, Batouche M, et al. Impact of La, Ni-doping on structural and electronic properties of $SrTiO_3$ for photocatalytic water splitting. Inorganic Chemistry Communications. 2023;153:110871.
43. Rusevich L, Kotomin E, Zvejnieks G, Popov A. Ab initio calculations of structural, electronic and vibrational properties of $BaTiO_3$ and SrTiO3

perovskite crystals with oxygen vacancies. Low Temperature Physics. 2020;46(12):1185-95.

44. Meyer R, Waser R, Helmbold J, Borchardt G. Observation of Vacancy Defect Migration in the Cation Sublattice of Complex Oxides by O 18 Tracer Experiments. Physical review letters. 2003;90(10):105901.
45. Dong X-L, Zhang K-H, Xu M-X. First-principles study of electronic structure and magnetic properties of $SrTi_{1-x}M_xO_3$ (M= Cr, Mn, Fe, Co, or Ni). Frontiers of Physics. 2018;13:1-7.
46. Hotovy I, Huran J, Spiess L. Characterization of sputtered NiO films using XRD and AFM. Journal of materials science. 2004;39(7):2609-12.
47. S. Piskunov, E. Heifets, R. I. Eglitis, and G. Borstel, "Bulk properties and electronic structure of SrTiO3, BaTiO3, PbTiO3 perovskites: an ab-initio HF/DFT study," *Comp. Mater. Sci.* **29**, p. 165, 2004.
48. Y. Zhu, J.M. Skelton, D.J. Lewis, R. Freer, Electronic transport and the thermoelectric properties of donor-doped $SrTiO_3$, Journal of Physics: Energy, 6 (2024) 025027.
49. Florez JM, Solis MA, Estay EAC, Morell ES, Ross CA. First-principles based Monte Carlo modeling of the magnetization of oxygen-deficient Fe-substituted SrTiO 3. Physical Chemistry Chemical Physics. 2023;25(28):19214-29.
50. Alarab F, Hricovini K, Leikert B, Richter C, Schmitt T, Sing M, et al. Nature of the metallic and in-gap states in Ni-doped $SrTiO_3$. APL Materials. 2024;12(1).
51. Li H, Tang Y, Yan W, Liu M, Wang Z, Li J, et al. Vacancy-enhanced photothermal activation for $CO_2$ methanation on $Ni/SrTiO_3$ catalysts. Applied Catalysis B: Environment and Energy. 2024;357:124346.